Singlet-triplet gaps in diradicals by the spin-flip approach: A benchmark study

Lyudmila V. Slipchenko and Anna I. Krylov
Department of Chemistry, University of Southern California, Los Angeles, California 90089-0482

(Received 14 May 2002; accepted 14 June 2002)

The spin-flip approach has been applied to calculate vertical and adiabatic energy separations between low-lying singlet and triplet states in diradicals. The spin-flip model describes both closed- and open-shell singlet and (low-spin) triplet states within a single reference formalism as spin-flipping, e.g., $\alpha \rightarrow \beta$, excitations from a high-spin triplet ($M_s=1$) reference state. Since both dynamical and nondynamical correlation effects are much smaller for the high-spin triplet states than for the corresponding singlet states, the spin-flip models yield systematically more accurate results than their traditional (non-spin-flip) counterparts. For all the diradicals studied in this work, the spin-flip variant of the coupled-cluster model with double excitations yields energy separations which are within less than 3 kcal/mol of the experimental or the highly accurate multireference values. In most cases the errors are about 1 kcal/mol. © *2002 American Institute of Physics.*
[DOI: 10.1063/1.1498819]

I. INTRODUCTION

Following Salem,[1] we can define diradicals as molecules with two electrons occupying two (near)-degenerate molecular orbitals. More loosely, Salem considers molecules with a broken bond as diradicals. Since chemical reactions involve bond breaking, diradicals as reaction intermediates or transition states are essential in interpreting mechanisms.[2–5]

Figure 1 shows the six Slater determinants which can be generated by distributing two electrons in two molecular orbitals. From these, three singlet, $\{\Psi_i^s\}_{i=1}^3$, and three triplet, $\{\Psi_i^t\}_{i=1}^3$, wave functions can be composed as follows:

$$\Psi_1^s = \tfrac{1}{2}[\lambda(\phi_1)^2 - \sqrt{1-\lambda^2}(\phi_2)^2](\alpha\beta - \beta\alpha), \quad (1)$$

$$\Psi_2^s = \tfrac{1}{2}[\lambda(\phi_1)^2 + \sqrt{1-\lambda^2}(\phi_2)^2](\alpha\beta - \beta\alpha), \quad (2)$$

$$\Psi_3^s = \tfrac{1}{2}(\phi_1\phi_2 + \phi_2\phi_1)(\alpha\beta - \beta\alpha), \quad (3)$$

$$\Psi_1^t = \tfrac{1}{2}(\phi_1\phi_2 - \phi_2\phi_1)(\alpha\beta + \beta\alpha), \quad (4)$$

$$\Psi_2^t = \tfrac{1}{\sqrt{2}}(\phi_1\phi_2 - \phi_2\phi_1)(\alpha\alpha), \quad (5)$$

$$\Psi_3^t = \tfrac{1}{\sqrt{2}}(\phi_1\phi_2 - \phi_2\phi_1)(\beta\beta). \quad (6)$$

Here $\phi_i\phi_j$ is a shorthand notation for the $\phi_i(1)\phi_j(2)$, and $\alpha\beta$ stands for the $\alpha(1)\beta(2)$. As dictated by the Pauli principle, the spatial parts of singlets are symmetric with respect to the interchange of two electrons, whereas the spatial parts of triplets are antisymmetric.

Much insight concerning the properties of diradicals has been derived from a simple analysis of these wave functions and their interactions.[1,3,4] For example, all two-electron triplet states are purely covalent, regardless of the nature of ϕ_1 and ϕ_2. This is consistent with the Pauli principle which does not allow two electrons with the same spin to coexist in the same volume of space, as required in ionic (or zwitterionic) configurations. When the orbitals ϕ_1 and ϕ_2 are nonbonding (heterosymmetric diradical,[1] e.g., the two p orbitals in methylene), the singlet Ψ_3^s is also covalent, whereas Ψ_1^s and Ψ_2^s are purely ionic wave functions. However, when the orbitals ϕ_1 and ϕ_2 constitute a bonding–antibonding pair (homosymmetric diradical,[1] e.g., π and π^* in twisted ethylene), the singlet Ψ_3^s state becomes purely ionic, while Ψ_1^s and Ψ_2^s can vary from purely ionic to purely covalent configurations.[6]

From a methodological point of view, however, it is important that all three singlet wave functions are of two-determinant form. When ϕ_1 and ϕ_2 are exactly degenerate, each singlet wave function consists of two equally important configurations. Therefore, the Hartree–Fock wave function, i.e., the single Slater determinant, is a qualitatively incorrect approximation for Ψ_{1-3}^s and Ψ_1^t. Only a multiconfigurational model which treats the important determinants on an equal footing, such as multiconfigurational self-consistent field (MCSCF),[7,8] provides an appropriate zero-order wave function for a diradical. To achieve quantitative accuracy, an appropriate zero-order wave function should be augmented by dynamical correlation, e.g., by configuration interaction (MRCI) or perturbation theory (MRPT). Multireference CI with single and double excitations (MR-CISD),[9] also known as second order CI (SOCI), complete active space SCF with second-order perturbation corrections (CASPT2),[10,11] or multiconfigurational quasidegenerate perturbation theory (MCQDPT2)[12] are the most commonly used methods of this type (see Ref. 13 for a comprehensive review of multireference methods). Recently, variants of multireference coupled-cluster (MRCC) and equation-of-motion coupled-cluster (EOM-CC) models targeting diradicals have been introduced by Nooijen and co-worker.[14,15]

The inclusion of dynamical correlation is crucial for a correct quantitative (and sometimes even qualitative) description of the electronic structure of diradicals.[16–19] Besides the well-known tendency of bare MCSCF wave functions to overestimate bond lengths and underestimate

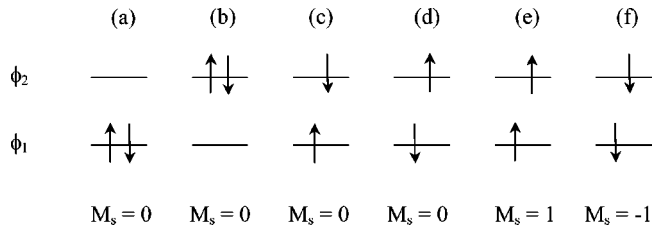

FIG. 1. Slater determinants which can be generated by distributing two electrons in two molecular orbitals. The projection of the total spin, M_s, is shown. Determinants (a)–(d) have $M_s=0$. Determinants (a) and (b) are also eigenfunctions of the $\hat{S}^2$ operator with expectation value zero (singlet). Note that these determinants always belong to the fully symmetric irreducible representation as they are of the closed-shell type. Therefore, they both can be present in fully symmetric singlet diradical's wave functions, i.e., Eqs. (1) and (2). $\langle \hat{S}^2 \rangle$ for the determinants (c) and (d) equals one. Their linear combinations are eigenfunctions of $\hat{S}^2$: (c)–(d) yields a singlet wave function [Eq. (3)], whereas (c)+(d) yields the $M_s=0$ component of a triplet [Eq. (4)]. Determinants (e) and (f) are high-spin $M_s=\pm 1$ components of the triplet state [Eqs. (5) and (6), respectively].

frequencies, the stationary points of the potential energy surface (PES) corresponding to diradicals can disappear at a higher level of theory.[19] Moreover, the balanced description of nondynamical and dynamical correlations requires active spaces much larger than the simple two-orbital one.[20]

To summarize, the theoretical description of singlet diradicals [Eqs. (1)–(3)] is difficult due to their multireference character. The triplet diradical wave functions, however, are much simpler. While the $M_s=0$ triplet wave function (4) is also two-configurational, the corresponding high-spin components (5) and (6) are of single-determinant form. Therefore, these states can be described by any single-reference method, the accuracy being systematically improved as one proceeds from the Hartree–Fock model towards correlated approaches. With respect to the high-spin [Eqs. (5) and (6)] triplet states, all singlet states [Eqs. (1)–(3)] as well as the $M_s=0$ component of the triplet [Eq. (4)] are formally *single-electron excitations involving spin-flip*. Thus, they can be described by the appropriate single-reference based excited state theory, e.g., by configuration interaction singles (CIS),[21–23] perturbatively corrected CIS, CIS(D),[24] or EOM-CC models, e.g., EOM-CC with singles and doubles (EOM-CCSD)[25,26] or EOM optimized-orbital coupled-cluster doubles (EOM-OO-CCD or simply EOM-OD).[27] This is the essence of the spin-flip (SF) approach.[28–30] *The SF model describes closed and open shell singlet states within a single-reference formalism as spin-flipping, e.g.,* $\alpha \rightarrow \beta$*, excitations from a triplet* ($M_s=1$) *reference state for which both dynamical and nondynamical correlation effects are much smaller than for the corresponding singlet state*.[28–30] By employing theoretical models of increasing complexity for the reference wave function, the description of the final states can be systematically improved. Thus, the SF method represents a robust tool for studying diradicals. It has been shown that the SF models describe the equilibrium properties of all three diradical states (1)–(3) with an accuracy comparable to that of traditional methods when applied to well behaved molecules.[29] The primary goal of this paper is to investigate the accuracy of the SF models for evaluating energy differences, e.g., singlet–triplet (ST) gaps in diradicals.

Since the diradical states (1)–(4) differ in their character (i.e., triplets are covalent while singlets may vary from purely covalent to purely ionic), it is not surprising that their chemical properties are also considerably different.[31] The small energy separation between these states makes them easily accessible in experiments, thereby allowing us to fine-tune the chemical properties of diradicals.[32] Determining the energy separation between triplet and low-lying singlet states of diradicals is the first step in understanding their chemical properties.

Most of the previously reported calculations of ST gaps have used MRCI or MRPT methods.[17–19,33–51] Due to the difficulties inherent in multireference techniques, the capability of highly correlated single reference models to describe some of the diradical states has raised a considerable enthusiasm: Schreiner and co-workers have reported applications[52,53] of Brueckner CCD[54] with perturbative account of the triples, B-CCD(T) method[55] (spin-symmetry broken solutions have been employed to describe Ψ_3^s, while Ψ_1^s has been modeled within a spin-restricted formalism). Moreover, a number of attempts have been made to generalize density functional theory (DFT) to treat multireference situations.[56–58]

The structure of the paper is as follows: The next section outlines the SF approach and computational details, Sec. III presents numerical examples for ST energy gaps in selected diradicals, and Sec. IV gives our concluding remarks.

II. THEORETICAL METHOD AND COMPUTATIONAL DETAILS

A. Theory

In traditional (non-SF) single-reference based excited-state models, the excited state wave functions are parametrized as follows:

$$\Psi^{s,t}_{M_s=0} = \hat{R}_{M_s=0} \tilde{\Psi}^s_{M_s=0}, \tag{7}$$

where $\tilde{\Psi}^s_{M_s=0}$ is a closed-shell reference wave function, and the operator $\hat{R}$ is an excitation operator truncated at a certain level of excitation (which should be consistent with the theoretical model employed to describe the reference $\tilde{\Psi}^s$). Note that only excitation operators which do not change the total number of α and β electrons, i.e., $M_s=0$, need to be considered in Eq. (7).

When the closed-shell reference $\tilde{\Psi}^s$ is well described by a single-reference wave function, the excited singlet and triplet states [including open-shell configurations, such as Eqs. (3) and (4)] are also well described by Eq. (7). However, the quality of the excited states $\Psi^{s,t}$ deteriorates when a single-reference description of $\tilde{\Psi}^s$ becomes inappropriate, as in the case of diradicals whose singlet states are two-configurational wave functions of type (1).

To overvcome this problem, the SF model employs a high-spin triplet reference state which is accurately described

by a single-reference wave function. The target states, closed- and open-shell singlets and triplets, are described as spin-flipping excitations:

$$\Psi^{s,t}_{M_s=0}=\hat{R}_{M_s=-1}\tilde{\Psi}^{t}_{M_s=+1}, \tag{8}$$

where $\tilde{\Psi}^{t}_{M_s=+1}$ is the $\alpha\alpha$ component of the triplet reference state, $\Psi^{s,t}_{M_s=0}$ stands for the final $(M_s=0)$ singlet and triplet states, respectively, and the operator $\hat{R}_{M_s=-1}$ is an excitation operator that flips the spin of an electron. As can be seen from Fig. 1, all the configurations used to describe diradical wave functions (1)–(4) are formally single excitations with respect to configuration (5). Therefore, the SF ansatz (8) is sufficiently flexible to describe both closed-shell and open-shell diradical states in a balanced fashion, i.e., without overemphasizing the importance of one of the configurations.

Similarly to traditional excited state theories, the description of the final states can be systematically improved by employing theoretical models of increasing complexity for the reference wave function. For example, the simplest SF model employs a Hartree–Fock wave function, and the operator $\hat{R}$ is then truncated at single excitations (SF-CIS or SF-SCF).[28] SF-CIS can be further augmented by perturbative corrections [SF-CIS(D) or SF-MP2].[29] A yet more accurate description can be achieved by describing the reference wave function by a coupled-cluster model, e.g., CCSD or OO-CCD. In this case, the excitation operator $\hat{R}$ consists of single and double excitation operators involving a flip of the spin of an electron.[28] The corresponding SF equations in spin–orbital form are identical to those of traditional excited state theories, i.e., CIS, CIS(D), or EOM-OD; however, they are solved in a different subspace of determinants: non-SF theories consider only $M_s=0$ excitation operators, whereas SF operates in the $M_s=-1$ subspace. The computational cost and scaling of SF models is identical to that of the corresponding non-SF excited state theories.

B. Computational details

Several considerations should be taken into account when calibrating electronic structure models.[59] A direct comparison to experiment is not always possible, in particular when short-lived transient species such as diradicals are concerned. For example, even for methylene, arguably the most studied diradical, the experimental data are very scarce for states other than the ground triplet and the lowest singlet states. Moreover, often it is not the *vertical* but the *adiabatic* (T_e) excitation energies which are reported. The dependence of T_e on equilibrium geometries of both states introduces additional uncertainties (vertical excitation energies are more useful for benchmark purposes, because they are calculated at the ground state equilibrium geometry). In addition, most of the experimentally measured energy separations are between the lowest vibrational states (T_{00}) and thus include changes in zero-point energies (ZPE). Lastly, it is important to separate the method from one-electron basis set effects. Unlike molecular geometries and frequencies, the convergence of energy differences with respect to the latter is rather slow.[59] That is why it is advantageous to benchmark a new theory against full configuration interaction (FCI) or other accurate models, e.g. MRCI or MRPT. In addition to addressing the basis set issue, this strategy enables the elimination of uncertainties due to equilibrium geometries and ZPEs.

With the above considerations in mind, we start our benchmark study by calculating singlet–triplet gaps in atoms, i.e., carbon, oxygen, and silicon. Since for atoms there is no uncertainty associated with equilibrium geometries and vibrational frequencies, the comparison with experiment is straightforward. Thus, these simple systems allow us to investigate the convergence of the SF models with respect to the one-particle basis set. We then proceed to a set of isovalent molecules with a varying diradical character, i.e., CH_2, NH_2^+, SiH_2, and PH_2^+. These diradicals are popular as benchmark systems,[33–39,41,60] because of their small size (but rich electronic structure), and the availability of experimental data.[61–66] For these systems, we compare the performance of the SF models against a variety of single- and multireference methods, and investigate the convergence of different methods with respect to the one-particle basis set. Next we consider a set of diatomic molecules with a diradical singlet state (NH, NF, OH^+, and O_2) for which accurate experimental data are available.[67] After thorough investigation of the performance of the SF method for these semimodel systems, we proceed to two important prototype diradicals: the benzyne isomers and trimethylenemethane (TMM). These systems, which are important in organic and bio-organic chemistry, have attracted the attention of both experimentalists and theoreticians.[18,42–48,52,68–72]

In order to minimize uncertainties due to equilibrium structures, we follow a commonly used strategy: adiabatic energies are estimated by using the best available structures, the same geometries being used for all the benchmarked methods. The choice of structures is specific for each system, and is discussed in the corresponding sections. For TMM, we also report vertical excitation energies, which are more suitable for benchmarking because they do not depend on excited states geometries.

To investigate one-particle basis set effects, we complement the calculations in relatively large basis sets by estimating the complete basis set (CBS) limiting values. Several procedures are employed: (i) two-point extrapolation (CBS-2p), which is based on cc-pVTZ and cc-pVQZ energies; (ii) two three-point extrapolations based on cc-pVDZ, cc-pVTZ, and cc-pVQZ energies: CBS-3pa and CBS-3pb; (iii) an energy separability scheme where basis set effects for a highly correlated model are evaluated by performing calculations with a less computationally expensive method.

The two-point procedure (i) extrapolates the asymptotic values of the total energies in the CBS limit (E_{CBS}) as follows:[59]

$$E_{\mathrm{CBS}}=E_X+AX^{-3}, \tag{9}$$

where X is the basis set cardinal number (i.e., $X=3$ for the cc-pVTZ basis, $X=4$ for the cc-pVQZ basis, etc.), E_X is the corresponding total energy,[73] and A is a fitting parameter defined such that Eq. (9) is satisfied for two bases (e.g., for $X=3$ and for $X=4$).

The three-point extrapolation, CBS-3pa, employs the following formula for the asymptotic behavior of the total energy:[74,75]

$$E_{\mathrm{CBS}} = E_X + B\exp(-CX). \tag{10}$$

The CBS-3pb three-point extrapolation suggested by Peterson and co-workers[76,77] is defined as:

$$E_{\mathrm{CBS}} = E_X + B\exp[-(X-1)] + C\exp[-(X-1)^2]. \tag{11}$$

In Eqs. (10) and (11), parameters B and C are defined such that the corresponding equations are satisfied for the three basis sets (e.g., $X=2$, $X=3$, and $X=4$).

In addition, we have also used an extrapolation technique based on an energy separability scheme:

$$E^{\mathrm{large}}_{\mathrm{SF\text{-}OD}} = E^{\mathrm{small}}_{\mathrm{SF\text{-}OD}} + (E^{\mathrm{large}}_{\mathrm{SF\text{-}CIS(D)}} - E^{\mathrm{small}}_{\mathrm{SF\text{-}CIS(D)}}), \tag{12}$$

where E^{large} and E^{small} refer to the total energies calculated in large (e.g., cc-pVTZ) and small (e.g., 6-31G*) basis sets. This procedure assumes that changes in the total energy due to the basis set increase are similar for the less and more correlated models [e.g., MP2 and CCSD, or SF-CIS(D) and SF-OD].

For all extrapolation procedures, the CBS values of singlet-triplet splittings are obtained by taking the differences between the extrapolated total energies of triplet and singlet states. Calculations are performed using two *ab initio* packages, Q-CHEM (Ref. 78) and PSI III,[79] to which our programs for SF-CIS, SF-CIS(D), and SF-OD calculations are linked. Additional results are obtained using the ACES II *ab initio* program.[80] Multireference calculations are performed using the GAMESS electronic structure package.[81] Some basis sets are obtained from the EMSL database.[82] All electrons are active in our calculations unless stated otherwise.

III. RESULTS AND DISCUSSION

When benchmarking *ab initio* methods, two aspects should be addressed: (i) the relative performance of methods with similar computational scaling and cost; and (ii) the absolute performance, e.g., the accuracy of a given method as compared against more computationally expensive but more accurate models. With this in mind, we compare the performance of the SF methods with (i) the corresponding non-SF approaches whose computational cost and scaling are identical [e.g., SF-CIS vs CIS, SF-CIS(D) versus CIS(D), SF-OD versus EOM-OD or EOM-CCSD]; and (ii) potentially more accurate methods which have higher computational cost [e.g., SF-OD vs CCSD(T)/B-CCD(T), or versus MRPT/MRCI]. Our results demonstrate that the performance of the SF models is systematically better than that of non-SF methods. On an absolute scale, it is comparable to that of the more computationally expensive multi-reference models.

The errors in ST energy gaps calculated by SF and single-reference non-SF methods are systematic. For example, in systems with a triplet ground state, the energy splittings between the triplet and the closed-shell singlet are overestimated, whereas for systems whose ground state is a closed-shell singlet the corresponding energy gaps are underestimated. The errors in the SF are systematically smaller in both cases, with the differences between the SF and non-SF models getting smaller as more correlated wave functions are employed for the reference. These trends can be easily rationalized by considering the two electrons in two-orbital model described in Sec. I.

Consider first the most straightforward approach, in which the energy separation between the lowest singlet and the lowest triplet states is computed as a difference between the total energies of the corresponding states calculated by a ground state method. For a molecule with a significant diradical character, the closed-shell singlet state Ψ^s_1 is poorly described by a single-reference wave function which fails to treat determinants (a) and (b) from Fig. 1 on an equal footing. Therefore, the resulting total energy of this state is too high. In contrast, the high-spin triplet states (Ψ^t_2 or Ψ^t_3) are better described by a single-reference method. That is why the triplet's total energy is too low relative to the singlet's, and the corresponding energy gap is too small for molecules with a singlet ground state, and too large for molecules with a triplet ground state. Sometimes even the ordering of states can be reversed. For example, Hartree–Fock calculations predict that the ground state of ozone is a triplet. The imbalance decreases as more correlated wave functions are employed (e.g., CCSD yields the correct multiplicity of the ground state; however, the energy gap is still grossly underestimated).

A more balanced description can be achieved by employing the corresponding excited state theory [see Eq. (7)], e.g., CIS in case of a Hartree–Fock reference wave function. However, since traditional (i.e., non-SF) single-reference methods employ a (poorly described) closed-shell singlet wave function Ψ^s_1 as the reference in excited state calculations, the ST gaps are still underestimated (for molecules with a singlet ground state). An additional advantage of using excited state theory to calculate ST gaps (as opposed to a direct energy differences approach) is that it can also describe other singlet states, e.g., the open-shell singlet Ψ^s_3 and the second closed-shell singlet Ψ^s_2. Note that a single-reference excited state theory will describe Ψ^s_3 and Ψ^t_1 in a more or less balanced fashion, since both states are formally single excitations from Ψ^s_1. Thus, the energy difference between Ψ^s_1 and Ψ^s_3 will also be underestimated. The second closed-shell singlet, Ψ^s_2, is formally a doubly excited state from the Ψ^s_1 reference. Therefore, it can only be described by methods that explicitly include double excitations (e.g., EOM-OD or EOM-CCSD). Moreover, the energy of this state will be too high relative to the singly excited states. To summarize, for a diradical with a triplet ground state (e.g., methylene), single-reference methods will (i) overestimate the ST energy separation between the triplet and the first closed-shell singlet; (ii) dramatically overestimate the energy gap between the triplet and the second closed-shell singlet; and (iii) underestimate the energy separation between the first closed-shell singlet and open-shell singlet, the relative ST gap between Ψ^t_1 and Ψ^s_3 being reproduced relatively well. When heavily correlated methods (e.g., EOM-OD) are employed, the description of all states is improved; however, the inherent imbalance in the non-SF single-reference wave

TABLE I. The energy separation between ^1D and ^3P states (eV) in carbon, oxygen, and silicon atoms.[a]

Basis	CIS	CIS(D)	EOM-OD	SF-CIS	SF-CIS(D)	SF-OD
			Carbon			
DZP[b]	1.645	1.478	1.520	1.484	1.472	1.462
TZ2P	1.662	1.432	1.490	1.457	1.423	1.417
TZ2P+diff	1.660	1.431	1.489	1.460	1.424	1.417
TZ2PF	1.656	1.348	1.385	1.415	1.341	1.314
TZ2PF+diff	1.654	1.346	1.385	1.417	1.342	1.314
TZ3P2F	1.654	1.320	1.353	1.401	1.315	1.281
cc-pVDZ				1.476	1.465	1.465
cc-pVTZ				1.413	1.342	1.316
cc-pVQZ	1.658	1.300	1.342	1.403	1.300	1.270
CBS-2p				1.396	1.270	1.236
CBS-3pa				1.407	2.310	2.355
CBS-3pb				1.399	1.276	1.244
			Oxygen			
DZP[b]	2.307	2.126	2.209	2.168	2.141	2.154
TZ2P	2.318	2.072	2.161	2.155	2.097	2.105
TZ2P+diff	2.317	2.071	2.161	2.158	2.099	2.107
TZ2PF	2.329	2.010	2.087	2.126	2.033	2.027
TZ2PF+diff	2.328	2.009	2.087	2.128	2.035	2.029
TZ3P2F	2.333	1.985	2.060	2.118	2.009	2.001
cc-pVDZ				2.152	2.124	2.131
cc-pVTZ				2.117	2.030	2.024
cc-pVQZ	2.334	1.963	2.041	2.116	1.990	1.981
CBS-2p				2.114	1.960	1.950
CBS-3pa				2.119	1.969	1.963
CBS-3pb				2.116	1.966	1.956
			Silicon			
TZ2P+diff	1.177	0.979	1.016	0.929	0.938	0.940
cc-pVTZ	1.196	0.880	0.881	0.863	0.827	0.793
cc-pVQZ	1.180	0.820	0.834	0.845	0.787	0.747

[a]Experimental values are 1.26 eV, 1.97 eV, and 0.75 eV for C, O, and Si, respectively [A. R. Striganov and N. S. Sventitskii, *Tables of Spectral Lines of Neutral and Ionized Atoms* (Plenum, New York, 1968)].
[b]FCI/DZP values are 1.471 eV for carbon and 2.166 eV for oxygen.

functions would result in rather large errors in the relative energies.

The SF models use a triplet high-spin state, e.g., Ψ_2^t, as a reference. Since this reference is accurately described by single-reference wave functions, and since all $M_s=0$ electronic configurations from Ψ_{1-3}^s and Ψ_1^t are formally single electron excitations from Ψ_2^t, all these states are described with similar accuracy. Thus, even though the ST gaps will still be overestimated (in a methylene-type diradical), the errors will be systematically smaller than these obtained in the corresponding non-SF methods.

A. ^3P-^1D energy gaps in carbon, oxygen, and silicon atoms

In atoms, there is no ambiguity due to geometries and ZPEs, and therefore the comparison between the calculated and experimental ST gaps is straightforward. In the following three examples, we compare the accuracy of the traditional excited state methods with that of the SF models. In order to elucidate basis set effects on the ST energy differences, we employ nine basis sets[83] and perform CBS extrapolations.[59,74–77]

For all three atoms, the ground state is a triplet ^3P state, and the lowest singlet is a ^1D state. Table I summarizes the ST energy gaps calculated by the traditional, i.e., non-SF, and

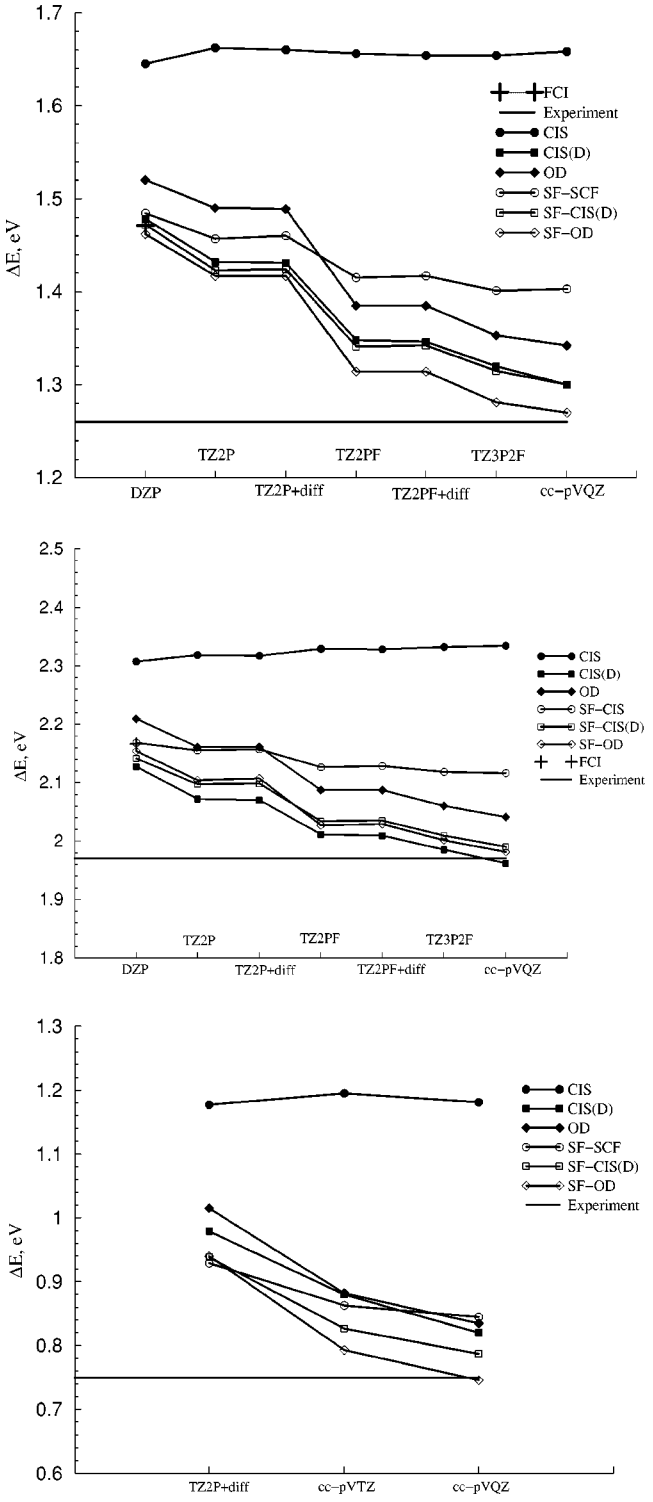

FIG. 2. Singlet-triplet energy separations in carbon (upper panel), oxygen (middle panel), and silicon (lower panel). The SF-OD/cc-pVQZ values are very close to the experimental ones. The SF models consistently yield more accurate results than the non-SF ones.

the SF methods. The convergence of ΔE_{ST} with respect to the basis set is illustrated in Figs. 2(a–c). Clearly, the SF results are consistently more accurate than those of the corresponding non-SF models. For example, the ST gaps calculated by the SF-CIS model are approximately 0.2 eV closer to the experimental values than those obtained by the CIS

method. The difference between the SF-OD and the EOM-OD results is about 0.06–0.09 eV, with the SF results being more accurate. The CIS(D) and SF-CIS(D) methods give similar values of ST gaps (in most basis sets, the differences are about 0.03 and 0.04 eV, less than 0.01 eV for oxygen, silicon, and carbon, respectively).

Figures 2(a)–2(c) demonstrates that the accurate description of the ground triplet state and the first excited singlet state (and the energy difference between them) requires basis sets with extensive polarization (e.g., f functions are very important), while diffuse functions do not affect the quality of the description. In the case of the less correlated methods (CIS and SF-CIS), the basis set convergence is fast. For the more correlated EOM-OD and SF-OD methods, large basis sets are crucial for obtaining converged results. In the largest basis set used, cc-pVQZ, the SF-OD results are within 0.01 eV of the experimental values. The SF-CIS(D) limiting values deviate from the experiment by no more than 0.04 eV (1 kcal/mol). For carbon and oxygen, we also estimate the CBS values of the ST energy differences by two-point and three-point extrapolations (see Sec. II B). For oxygen, all the approximations give similar results: the CBS values of E_{ST} for the SF-OD method are about 0.02 eV lower than the experimental value. However, the discrepancy between the different models is much larger in the case of carbon: while the CBS-2p and CBS-3pb values are reasonable, the CBS-3pa extrapolation fails. This is because our CBS-3pa procedure uses cc-pVDZ total energies which are apparently too far from the CBS limit, in order for the extrapolation formula (10) to be justified. Note that whereas the values of the ST gaps calculated in cc-pVDZ basis are reasonable, CBS-3pa which uses cc-pVDZ total energies, yields inconsistent results. The CBS-3pb extrapolation appears to be more robust: even though it also uses the cc-pVDZ total energies, it yields consistent results which agree well with the CBS-2p ones. As in the case for oxygen, the CBS-3pb extrapolated SF-OD value of E_{ST} in carbon is 0.02 eV lower than the experimental value.

B. Methylene and other isovalent molecules

The electronic structure of the isovalent CH_2, NH_2^+, SiH_2, and PH_2^+ molecules is qualitatively described in Fig. 1. The orbitals ϕ_1 and ϕ_2 (see Fig. 1) are derived from a p-orbital and a $s^{1-x}p^x$-hybridized orbital of the heavy atom, respectively. Thus, in Salem classification, these species are heterosymmetric diradicals (except for the linear geometry).[1] The symmetries of the (nearly) degenerate ϕ_1 and ϕ_2 are (i) $3a_1$ and $1b_1$ in CH_2 and NH_2^+ and (ii) $5a_1$ and $2b_1$ in SiH_2 and PH_2^+. The energy gap between ϕ_1 and ϕ_2 gradually changes in these series. This tunable diradical character along with the small size of these species makes them very attractive model systems for both experimental[61–66] and theoretical[33–39,41,60] studies.

The ground state of methylene (CH_2) and the nitrenium ion (NH_2^+) is the triplet state $\tilde{X}\,^3B_1$ whose electronic configuration is described by Eqs. (4)–(6):

$$\tilde{X}\,^3B_1 \approx (1a_1)^2(2a_1)^2(1b_2)^2(1b_1)(3a_1). \tag{13}$$

The first excited state is a closed-shell singlet $\tilde{a}\,^1A_1$ state, i.e., Ψ_1^s of Eq. (1):

$$\tilde{a}\,^1A_1 \approx \lambda(1a_1)^2(2a_1)^2(1b_2)^2(3a_1)^2 - \sqrt{1-\lambda^2}(1a_1)^2(2a_1)^2(1b_2)^2(1b_1)^2. \tag{14}$$

The second excited singlet state is an open-shell singlet $\tilde{b}\,^1B_1$, i.e., Ψ_3^s of Eq. (3), whose electronic configuration is similar to that of the triplet state of Eq. (13). The third excited state is a closed-shell singlet $\tilde{c}\,^1A_1$ of Ψ_2^s type [Eq. (2)]:

$$\tilde{c}\,^1A_1 \approx \lambda(1a_1)^2(2a_1)^2(1b_2)^2(1b_1)^2 + \sqrt{1-\lambda^2}(1a_1)^2(2a_1)^2(1b_2)^2(3a_1)^2. \tag{15}$$

This state has the same symmetry as the lowest singlet and is formally a double excitation from the $\tilde{a}\,^1A_1$ state.

At linear geometries, the ϕ_1 and ϕ_2 orbitals become exactly degenerate, and the coefficient λ reaches its minimum value of $1/\sqrt{2}$. In this case, the proper labels are $\tilde{c}\,^1\Sigma_g^+$ for the second closed-shell singlet [Eq. (15)], and $^1\Delta_g$ for the first closed-shell and the open-shell singlet states, which then become exactly degenerate. (For example, the equilibrium geometry of the second closed-shell singlet state of NH_2^+ is linear, and therefore the $\tilde{c}\,^1\Sigma_g^+$ label is used.)

As explained by the Walsh correlation diagrams,[84] SiH_2 and PH_2^+ favor a closed-shell Ψ_1^s singlet as their ground state:

$$\tilde{X}\,^1A_1 \approx \lambda[\mathrm{core}](4a_1)^2(2b_2)^2(5a_1)^2 - \sqrt{1-\lambda^2}[\mathrm{core}](4a_1)^2(2b_2)^2(2b_1)^2, \tag{16}$$

where

$$[\mathrm{core}] = (1a_1)^2(2a_1)^2(1b_2)^2(3a_1)^2(1b_1)^2. \tag{17}$$

The first excited state in SiH_2 and PH_2^+ is the triplet $\tilde{a}\,^3B_1$ state, whose electronic configuration is:

$$\tilde{a}\,^3B_1 \approx [\mathrm{core}](4a_1)^2(2b_2)^2(5a_1)(2b_1). \tag{18}$$

The next state is an open-shell singlet $\tilde{A}\,^1B_1$, whose electronic configuration is similar to that of the $\tilde{a}\,^3B_1$ triplet from Eq. (18). Finally, the $\tilde{B}\,^1A_1$ state has the following electronic configuration:

$$\tilde{B}\,^1A_1 \approx \lambda[\mathrm{core}](4a_1)^2(2b_2)^2(2b_1)^2 + \sqrt{1-\lambda^2}[\mathrm{core}](4a_1)^2(2b_2)^2(5a_1)^2. \tag{19}$$

The systematic changes in the diradical character of these species, their ground state multiplicities, and equilibrium geometries can be rationalized by using the Walsh diagrams and Hund rules. By using hybridization theory, Walsh correlates the energy of the four valence orbitals with the H–X–H angle. The two bonding (σ_{XH}) and two nonbonding (ϕ_1 and ϕ_2) orbitals derive from the s and three p orbitals of the heavy atom. At linear geometry, the bonding orbitals are sp hybrids, whereas the nonbonding ones are the exactly degenerate nonhybridized p orbitals. Since the energy of the valence s orbital is lower than that of the p orbitals, the increased s character lowers the energy of a hybridized orbital. At 90°, the two σ_{XH} orbitals are unhybridized p orbit-

TABLE II. Total energies (hartree) for the ground $\tilde{X}\,^3B_1$ state of CH_2, and adiabatic excitation energies (eV) for the three singlet states.[a]

Method	$\tilde{X}\,^3B_1$	$\tilde{a}\,^1A_1$	$\tilde{b}\,^1B_1$	$\tilde{c}\,^1A_1$
SF-CIS/TZ2P	−38.93254	0.883	1.875	3.599
SF-CIS(D)/TZ2P	−39.05586	0.613	1.646	2.953
SF-OD/TZ2P	−39.08045	0.514	1.564	2.715
CASSCF SOCI/TZ2P (Ref. 33)	−39.064939	0.482	1.558	2.697
FCI/TZ2P (Ref. 60)	−39.066738	0.483	1.542	2.674
SF-CIS/TZ2P(f,d)	−38.93301	0.878	1.839	3.590
SF-CIS(D)/TZ2P(f,d)	−39.06782	0.577	1.579	2.882
SF-OD/TZ2P(f,d)	−39.09229	0.480	1.495	2.647
CASSCF SOCI/TZ2P(f,d) (Ref. 33)	−39.076865	0.440	1.486	2.620
SF-CIS/TZ2P(f,d)+diff	−38.93312	0.872	1.838	3.582
SF-CIS(D)/TZ2P(f,d)+diff	−39.06807	0.572	1.577	2.872
SF-OD/TZ2P(f,d)+diff	−39.09253	0.474	1.492	2.637
CASSCF SOCI/TZ2P(f,d)+diff (Ref. 33)	−39.076983	0.434	1.483	2.608
SF-CIS/TZ3P($2f,2d$)	−38.93326	0.865	1.822	3.592
SF-CIS(D)/TZ3P($2f,2d$)	−39.07201	0.551	1.551	2.864
SF-OD/TZ3P($2f,2d$)	−39.09613	0.454	1.464	2.636
CASSCF SOCI/TZ3P($2f,2d$) (Ref. 33)	−39.080240	0.411	1.450	2.595
SF-CIS/cc-pVDZ	−38.92152	0.876	1.933	3.723
SF-CIS(D)/cc-pVDZ	−39.01685	0.615	1.747	3.157
SF-OD/cc-pVDZ	−39.04117	0.524	1.677	2.918
SF-CIS/cc-pVTZ	−38.93226	0.869	1.845	3.629
SF-CIS(D)/cc-pVTZ	−39.06389	0.578	1.579	2.906
SF-OD/cc-pVTZ	−39.08793	0.483	1.495	2.674
SF-CIS/cc-pVQZ	−38.93471	0.864	1.826	3.603
SF-CIS(D)/cc-pVQZ	−39.08758	0.541	1.527	2.826
SF-OD/cc-pVQZ	−39.11097	0.451	1.447	2.612
SF-CIS/CBS-2p	−38.93651	0.860	1.812	3.583
SF-CIS(D)/CBS-2p	−39.10487	0.514	1.490	2.767
SF-OD/CBS-2p	−39.12779	0.427	1.412	2.567
SF-CIS/CBS-3pa	−38.93544	0.861	1.821	3.593
SF-CIS(D)/CBS-3pa	−39.11162	0.464	1.535	2.829
SF-OD/CBS-3pa	−39.13335	0.395	1.470	2.647
SF-CIS/CBS-3pb	−38.93600	0.861	1.816	3.588
SF-CIS(D)/CBS-3pb	−39.10197	0.517	1.498	2.780
SF-OD/CBS-3pb	−39.12493	0.430	1.420	2.579
Expt. (Ref. 61)		0.390	1.425	

[a]FCI/TZ2P optimized geometries (Refs. 60 and 86).

als, whereas the nonbonding orbitals ϕ_1 and ϕ_2 become the unhybridized s and p orbitals, respectively. In the diradicals' states discussed in this section, the σ_{XH} orbitals are always doubly occupied and therefore can be excluded from further discussion. The Ψ_1^s state is dominated by a configuration in which the two remaining electrons are placed on the ϕ_1 orbital, which is stabilized at small H−X−H angles. The open-shell Ψ_3^s and Ψ_{1-3}^t states favor larger angles, since both ϕ_1 and ϕ_2 host one electron. Finally, the second closed-shell singlet in which ϕ_2 is doubly occupied favors the largest H−X−H angles (up to 180°, as in NH_2^+).

In order to explain the changes in the diradical character, and the relative ordering of the first closed-shell singlet and lowest triplet states, the molecular geometries and charge distributions must be considered. As dictated by electronegativity considerations and covalent atomic radii, the X−H bond length increases in the following order: $NH_2^+ \rightarrow CH_2 \rightarrow PH_2^+ \rightarrow SiH_2$. The destabilization of small H−X−H angles decreases in the same order, because the repulsion between hydrogen atoms is larger for short bond lengths. At large angles, when ϕ_1 and ϕ_2 are almost degenerate, the Hund rule favors a triplet coupling, and this is why the ground state of NH_2^+ and CH_2 is a triplet. At small angles, when the energy gap between ϕ_1 and ϕ_2 is large, one-electron energetic considerations prevail, and a closed-shell singlet becomes the ground state (PH_2^+ and SiH_2). To summarize, the degeneracy between the nonbonding orbitals decreases in the above sequence, and therefore the diradical character increases in the reverse order: $SiH_2 \rightarrow PH_2^+ \rightarrow CH_2 \rightarrow NH_2^+$.

Calculations are performed using eight basis sets.[85] The geometries used to calculate adiabatic energy separations are summarized in Ref. 86.

1. CH_2

Since experimental geometries[61,87,88] are not available for all four diradical states of CH_2, we calculate adiabatic excitation energies at the FCI/TZ2P optimized geometries.[60,86] The SF models accurately describe the equilibrium properties of all these states, with the SF-OD geometries and frequencies being very close to those of FCI.[29]

Table II compares the adiabatic ST energy gaps calcu-

lated by the SF models and by CASSCF SOCI.[33] As explained above, the SF models systematically overestimate ΔE_{ST}, the errors being smallest for the $\tilde{X}\,^3B_1-\tilde{b}\,^1B_1$ splittings. The absolute errors of the SF models against CASSCF SOCI are rather small: SF-CIS overestimates the adiabatic excitation energy for the $\tilde{b}\,^1B_1$ state by 0.37 eV, and for both $^1A_1$ states by 1.00 eV. As more correlated SF models are used, these errors become smaller: 0.10–0.25 eV for SF-CIS(D), and 0.01–0.04 eV for SF-OD. Thus, for methylene the SF-OD results are within 1 kcal/mol of those of CASSCF SOCI.

Figure 3 presents the calculated $\Delta E_{\tilde{X}\,^3B_1-\tilde{a}\,^1A_1}$ as a function of the one-particle basis set. The convergence of the SF-CIS model is rather fast. However, for correlated wave functions very large bases are needed for the converged results. As Fig. 3 and Table II demonstrate, heavy polarization (e.g., three sets of d-functions and two sets of f-functions) is necessary for accurate results. On the other hand, diffuse functions, an increase in n-ζ beyond TZ, and polarization beyond f-functions are less important. For example, the SF-OD results in the TZ3P(2f,2d) basis are within 0.02 eV of the SF-OD/cc-pVQZ values [cc-pVQZ basis has the same number of f- and d-functions as TZ3P(2f,2d), but it also contains one set of g-functions on carbon and one set of f-functions of hydrogen]. The less extensive cc-pVTZ basis, which contains two sets of d-functions and one set of f-functions on carbon, yields results within 0.06 eV of our largest basis set, cc-pVQZ. We have also estimated the CBS limiting values of the ST gaps (see Sec. II B for details). As in the case of carbon (Sec. III A), the three-point extrapolation CBS-3pa breaks down for the $\tilde{X}\,^3B_1-\tilde{b}\,^1B_1$ and the $\tilde{X}\,^3B_1-\tilde{c}\,^1A_1$ transitions. The ΔE_{ST} estimated by the two-point procedure CBS-2p are suspiciously low. The three-point extrapolation CBS-3pb gives reasonable values for ΔE_{ST} for all transitions. Thus, the methylene results confirm the conclusions based on the results from Sec. II B: (i) the CBS extrapolation procedures should be used carefully in bases smaller than quintuple-ζ quality; (ii) CBS-3pb [Eq. (11)] is more robust than CBS-3pa [Eq. (10)] when using the cc-pVDZ/cc-pVTZ/cc-pVQZ results.

The assessment of the accuracy of the SF models against the experiment is less straightforward. The SF-OD/cc-pVQZ results for the first and second singlet states deviate from the experimental values by 0.061 and 0.022 eV, respectively. The SF-CIS(D)/cc-pVQZ numbers are off by 0.15 and 0.10 eV. However, since the experimentally measured value is the energy separation between the zero-point vibrational levels, it includes changes in ZPEs. These changes, estimated by using CISD frequencies,[33] are about 0.017 and 0.005 eV for the $\tilde{X}\,^3B_1-\tilde{a}\,^1A_1$ and the $\tilde{X}\,^3B_1-\tilde{b}\,^1B_1$ transitions, respectively. Therefore, the ZPE-corrected SF-OD/cc-pVQZ values are within 0.044 and 0.017 eV of the experiment (i.e., 1.0 and 0.4 kcal/mol, respectively). The SF-OD values, obtained by using the most stable CBS-3pb extrapolation, deviate by 0.040 and 0.005 eV from the experimental values, and when including ZPE corrections, they are within 0.023 and 0.010 eV from the experiment.

Table III compares the SF results against traditional (non-SF) methods. The TZ2P basis is used to enable comparison against the FCI results.[60] While in the FCI calculations one core and one virtual orbitals have been frozen, all electrons/orbitals are active in present calculations.

The first three rows in the Table III present the ST gaps computed by the least balanced approach, e.g., by taking the difference between the total energies for the triplet and singlet states calculated by the ground-state models. Here we consider the SCF, CCSD, and CCSD(T) methods. Note that such a procedure is not capable of describing the open-shell $\tilde{b}\,^1B_1$ singlet. In general, it can be applied only to calculate the energy gap between the lowest triplet and the lowest closed-shell-type singlet state. However, in this case it is also possible to evaluate the energy of the second A_1 singlet state [even though this state is of the same symmetry as the lowest singlet, the symmetries of orbitals in the reference determinant are different, e.g., $(1a_1)^2(2a_1)^2(1b_2)^2(3a_1)^2$ is the Hartree–Fock determinant for the $\tilde{a}^1A_1$ state, whereas $(1a_1)^2(2a_1)^2(1b_2)^2(1b_1)^2$ for $\tilde{c}^1A_1$]. Due to the inherently unbalanced treatment of the singlet and triplet states by single-reference wave functions, only the correlated CCSD and CCSD(T) methods yield accurate results for ΔE_{ST} for $\tilde{a}\,^1A_1$ (errors against FCI are 0.063 and 0.022 eV, respectively). However, both methods are about 0.7 eV off for the $\tilde{c}\,^1A_1$ state.

The next two rows in the Table III present results for the B-CCD and B-CCD(T) models [the computational cost of B-CCD/B-CCD(T) is similar to that of the CCSD/CCSD(T) models]. Following the approach of Schreiner and co-workers,[52,53] the triplet state energy is calculated by using the spin-unrestricted wave function, the closed-shell singlet's energy by using the spin-restricted wave function, and the energy of the open-shell singlet by using the spin-unrestricted spin-contaminated wave function. As expected, the B-CCD/B-CCD(T) results are almost identical to those of CCSD/CCSD(T)—both in terms of total energies and energy differences. Thus, for the $\tilde{a}\,^1A_1$ state the B-CCD/B-CCD(T) errors against FCI are 0.063/0.022 eV, respectively. The excitation energy for the open-shell singlet state, however, is about 1 eV off. Moreover, by definition[89] this approach will almost always place the open-shell singlet below the closed-shell one, thus reversing the states' ordering in methylene.

The next four rows in Table III present a more balanced approach than the direct energy difference one, that is, when the ST gaps are calculated by using single-reference excited state theories. Even though the closed-shell reference description of the lowest singlet state is not very accurate in methylene, the cancellation of errors results in improved values of the ST splittings. For example, the CIS value is closer to FCI by 0.25 eV than the value calculated by SCF energy differences. In the case of the correlated CCSD model, the improvement is less dramatic: 0.007 eV (thus, EOM-CCSD error equals 0.055 eV). More importantly, however, is that the excited state models can also describe the open-shell singlet state. Moreover, models which explicitly include double excitations (e.g., EOM-OD or EOM-CCSD) can even describe the second closed-shell singlet, even though such description is not very accurate (e.g., the EOM-OD values are more than 1 eV off).

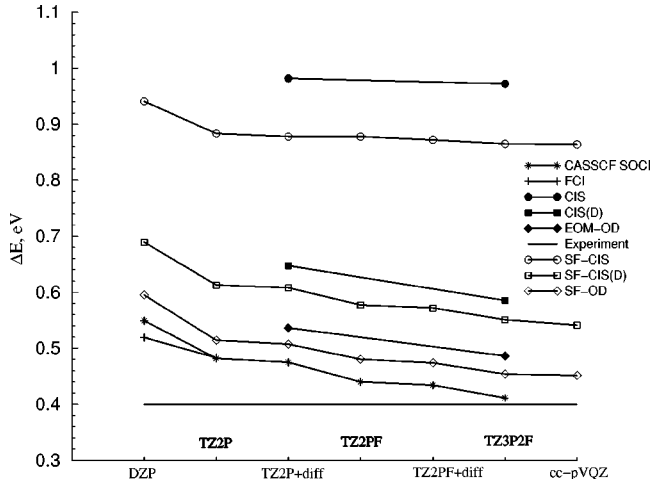

FIG. 3. Basis set dependence of the energy gap between the $\tilde{a}\,^1A_1$ and $\tilde{X}\,^3B_1$ states in methylene. E_{ST} values calculated by the single-reference (SF and non-SF) and multireference (CASSCF SOCI) methods are compared against the experimental value. For the DZP and TZ2P bases, the FCI results are also shown. The convergence of the E_{ST} values with respect to the basis set is rather slow for the highly correlated models, e.g., EOM-OD, SF-OD, and the CASSCF SOCI. SF results are consistently closer to the experimental value (and that of the CASSCF SOCI) than those of the corresponding single-reference non-SF methods.

By using the SF approach, the accuracy of single-reference theories is considerably improved. Moreover, all three singlet states can now be described with a similar accuracy. For example, the SF-CIS error for the lowest singlet is 0.11 eV smaller than that of the CIS. Moreover, the second closed-shell singlet, which is not accessible by the non-SF CIS, is now described with roughly the same accuracy as the other states. The SF-OD results are within 0.04 eV from the FCI ones for all three singlet states. As Fig. 3 demonstrates, this difference between the SF and non-SF models is systematic: regardless of the basis set used, all SF models are closer to the experimental value than the corresponding non-SF approaches.

2. NH_2^+

Table IV presents the adiabatic energy separations between the ground triplet $\tilde{X}\,^3B_1$ state and the three low-lying singlet states of NH_2^+ calculated in the TZ2P(f,d) basis set at the CISD/TZ2P(f,d) optimized geometries.[34,86] The difference between SF-OD and CASSCF SOCI[34] does not exceed 0.04 eV. By including the ZPE corrections estimated by using CISD frequencies,[34] the SF-OD value for the $\tilde{X}\,^3B_1-\tilde{a}\,^1A_1$ transition is within 0.02 eV from the experimental result.[62] The SF-CIS(D) error is also small and equals 0.08 eV.

TABLE III. Total energies (hartree) for the ground $\tilde{X}\,^3B_1$ state of CH_2, and adiabatic excitation energies (eV) for the three singlet states.[a]

	$\tilde{X}\,^3B_1$	$\tilde{a}\,^1A_1$	$\tilde{b}\,^1B_1$	$\tilde{c}\,^1A_1$
SCF	−38.937956	1.236		2.772
CCSD	−39.080919	0.545		2.054
CCSD(T)	−39.083856	0.505		1.907
B-CCD	−39.080815	0.545	0.467	2.054
B-CCD(T)	−39.083859	0.505	0.315	1.907
CIS	−38.92886	0.989	1.748	
CIS(D)	−39.05823	0.655	1.506	
EOM-CCSD	−39.08066	0.538	1.566	3.843
EOM-OD	−39.08077	0.543	1.569	3.847
SF-CIS/TZ2P	−38.93254	0.883	1.875	3.599
SF-CIS(D)/TZ2P	−39.05586	0.613	1.646	2.953
SF-OD/TZ2P	−39.08045	0.514	1.564	2.715
FCI (Ref. 60)	−39.066738	0.483	1.542	2.674

[a]FCI/TZ2P optimized geometries (Refs. 60 and 86).

TABLE IV. Total energies (hartree) for the ground states of NH_2^+, SiH_2, and PH_2^+, and adiabatic excitation energies (eV) for the three low-lying states.[a]

NH_2^+	$\tilde{X}\,^3B_1$	$\tilde{a}\,^1A_1$	$\tilde{b}\,^1B_1$	$\tilde{c}\,^1A_1$ ($\tilde{c}\,^1\Sigma_g^+$)
SF-CIS	−55.22731	1.673	2.151	4.375
SF-CIS(D)	−55.37545	1.342	1.959	3.635
SF-OD	−55.40259	1.305	1.941	3.419
CASSCF SOCI[b]	−55.388368	1.281	1.935	3.380
Expt.		1.306±0.010[c]		
SiH_2	$\tilde{X}\,^1A_1$	$\tilde{a}\,^3B_1$	$\tilde{A}\,^1B_1$	$\tilde{B}\,^1A_1$
SF-CIS	−290.03701	0.503	2.199	3.945
SF-CIS(D)	−290.27260	0.776	2.122	3.850
SF-OD	−290.29961	0.866	1.994	3.537
CASSCF SOCI[b]	−290.166351	0.871	1.992	3.486
Expt.		−0.91±0.03[d]	1.928[e]	
PH_2^+	$\tilde{X}\,^1A_1$	$\tilde{a}\,^3B_1$	$\tilde{A}\,^1B_1$	$\tilde{B}\,^1A_1$
SF-CIS	−341.55130	0.388	2.166	4.541
SF-CIS(D)	−341.71948	0.682	2.134	4.015
SF-OD	−341.74916	0.761	2.015	3.728
CASSCF SOCI[b]	−341.695054	0.760	2.009	3.686
Expt.[f]		−0.75±0.05	1.92	

[a]CISD/TZ2P(f,d) optimized geometries (Refs. 34–36, 86), TZ2P(f,d) basis set.
[b]CASSCF SOCI values are from Refs. 34–36.
[c]Reference 62.
[d]Reference 63.
[e]Reference 66.
[f]Reference 64.

3. SiH_2

Table IV shows the adiabatic energy separations between the ground and three excited states of SiH_2. The CISD/TZ2P(f,d) optimized geometries and the TZ2P(f,d)

TABLE V. Singlet–triplet ($^1\Delta$-$^3\Sigma$) adiabatic energy separations (eV) in selected diatomic molecules.[a]

	Basis	SF-CIS	SF-CIS(D)	SF-OD	Expt. (Ref. 67)
NH	cc-pVTZ	1.778	1.661	1.658	1.558
	cc-pVQZ	1.764	1.611	1.605	
NF	cc-pVTZ	1.775	1.570	1.527	1.487
	cc-pVQZ	1.770	1.531	1.491	
OH^+	cc-pVTZ	2.329	2.223	2.237	2.190
	cc-pVQZ	2.323	2.178	2.189	
O_2	cc-pVTZ	1.445	1.089	1.076	0.980
	cc-pVQZ	1.447	1.067	1.061	

[a]Experimental geometries used (Refs. 67 and 91).

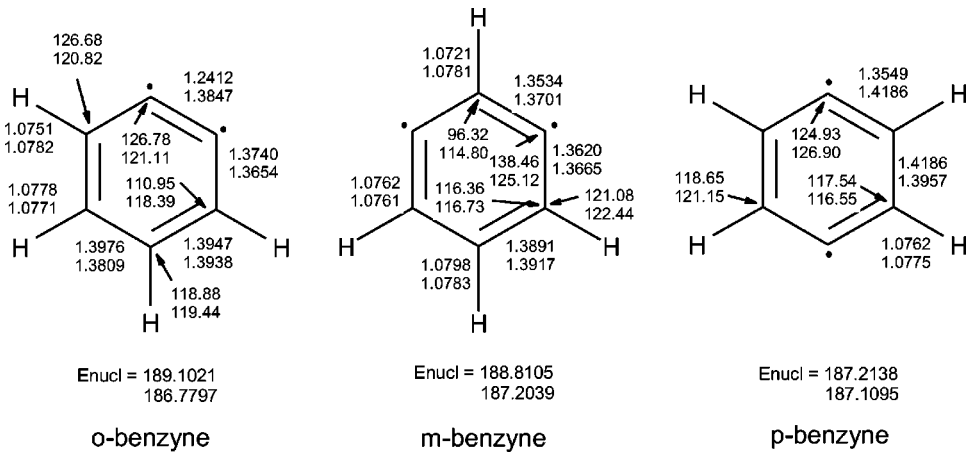

FIG. 4. Equilibrium geometries for the singlet (upper values) and triplet (lower values) states of benzynes (bond lengths are in angstroms, angles are in degrees, and nuclear repulsion energies are in hartrees). Structures are optimized at the SF-DFT/6-311G* level.

basis,[85] have been used.[35,86] As in the previous cases, SF-OD agrees very well with CASSCF SOCI.[35] The difference is less than 0.01 eV for the $\tilde{X}\,^1A_1-\tilde{a}\,^3B_1$ and $\tilde{X}\,^1A_1-\tilde{A}\,^1B_1$ transitions, and 0.05 eV for the $\tilde{X}\,^1A_1-\tilde{B}\,^1A_1$ one. The ZPE corrected[35] SF-OD value for the $\tilde{X}\,^1A_1-\tilde{a}\,^3B_1$ transition is within the experimental error.[63] The corresponding value for the $\tilde{X}\,^1A_1-\tilde{A}\,^1B_1$ transition is within 0.07 eV from the experiment.[66]

4. PH_2^+

CISD/TZ2P(f,d) optimized geometries[36,86] and a TZ2P(f,d) basis[85] have been used to calculate the adiabatic excitation energies in PH_2^+. Table IV compares the SF results against the CASSCF SOCI ones,[36] and the experiment.[64] As in the case of SiH_2, there is excellent agreement between the SF-OD and CASSCF SOCI results, the largest difference being 0.04 eV for the $\tilde{X}\,^1A_1-\tilde{A}\,^1B_1$ transition. The available experimental data are not very accurate.[64] However, they are in overall agreement with the theoretical values.

C. Diatomic molecules with a diradical singlet state

The set of diatomic molecules with a diradical singlet state (NH, NF, OH^+, and O_2) have been studied using the cc-pVTZ and cc-pVQZ bases.[90] The adiabatic $^1\Delta$-$^3\Sigma$ excitation energies are calculated by using experimental geometries.[67,91] Table V compares the SF results with the experimental values.[67,91] Overall, the agreement between the SF models and the experiment is very good: the SF-OD/cc-pVQZ results for NF and OH^+ are within 0.01 eV from the experiment, whereas for NH and O_2 the deviation is about 0.05 and 0.08 eV. The SF-CIS(D) numbers are within 0.04 eV from the SF-OD ones.

D. Benzyne

The ground state of the benzyne isomers is a closed-shell singlet state of Ψ_1^s type [Eq. (1) from Sec. I]: $^1A_1$ in C_{2v} (*o*- and *m*-benzynes) and ^1A_g in D_{2h} (*p*-benzyne) symmetries. The lowest excited state is a triplet state: $^3B_2$ in *o*- and *m*-benzynes, and $^3B_{1u}$ in *p*-benzyne (see Ref. 71 for analysis of the molecular orbitals in *p*-benzyne). The diradical character increases as the distance between the unpaired electrons

TABLE VI. Ortho-, meta-, and para-benzynes. Total ground-state energies (hartree) and adiabatic excitation energies (eV) to the lowest triplet state.[a]

	o-benzyne		*m*-benzyne		*p*-benzyne	
	$^1A_1$	$^3B_2$	$^1A_1$	$^3B_2$	^1A_g	$^3B_{1u}$
SF-DFT[b]	−230.77510	1.872	−230.74779	0.954	−230.72285	0.167
SF-CIS/6-31G*	−229.42629	0.960	−229.40348	0.118	−229.39737	0.014
SF-CIS(D)/6-31G*	−230.14905	1.406	−230.08006	0.701	−230.10905	0.095
SF-OD/6-31G*	−230.19490	1.490	−230.17066	0.696	−230.15415	0.174
SF-CIS/cc-pVTZ[c]	−229.49504	1.007	−229.47187	0.166	−229.46472	0.014
SF-CIS(D)/cc-pVTZ[c]	−230.45684	1.548	−230.38757	0.842	−230.41234	0.092
SF-OD/cc-pVTZ[c,d]	−230.50269	1.632	−230.47817	0.837	−230.45743	0.171
Expt. (Ref. 72)		1.628±0.013		0.911±0.014		0.165±0.016
Δ ZPE[e]		−0.028		0.043		0.021
Expt.−Δ ZPE		1.656		0.868		0.144

[a]SF-DFT/6-311G* optimized geometries (see Fig. 4).
[b]6-311G* basis.
[c]cc-pVTZ basis on carbon and cc-pVDZ basis on hydrogen.
[d]Estimated using Eq. (12).
[e]Calculated at the SF-DFT/6-311G* level.

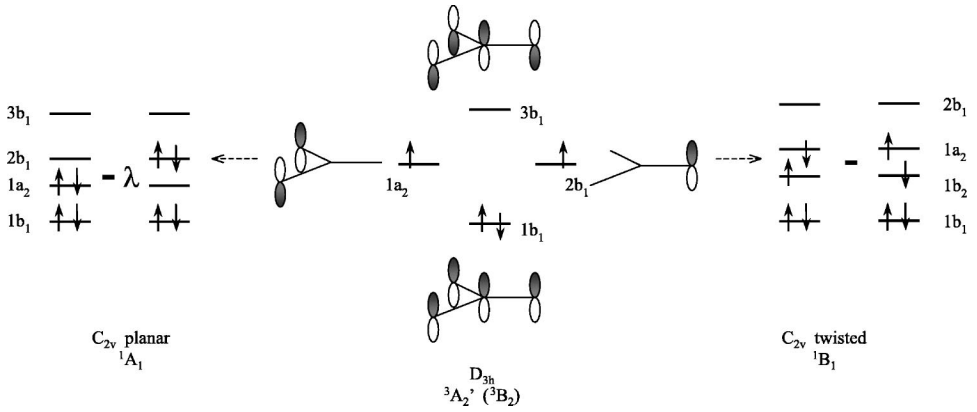

FIG. 5. The π system of TMM and the electronic configurations of the three lowest states. C_{2v} labels are used at the ground state equilibrium geometry (D_{3h}), where the $1a_2$ and $2b_1$ orbitals are two degenerate e' components. Two different distortions can lift the degeneracy between these orbitals (and the two lowest excited states, i.e., $^1A_1$ and $^1B_2$): one is a C_{2v} distortion, which leaves the molecule planar, whereas another involves a 90° rotation of one of the CH_2 groups. The former distortion stabilizes the $1a_2$ orbital and the closed-shell $^1A_1$ singlet state (shown on the left), whereas the latter favors the $2b_1$ orbital and the open-shell $^1B_2$ singlet state (shown on the right). Note that at the twisted C_{2v} geometry, the b_1 and b_2 labels interchange.

increases in the ortho→meta→para sequence. The increase in diradical character results in a singlet-triplet energy gap decrease in the same order. The strong diradical character of the singlet *p*-benzyne results in orbital instabilities for the singlet state.[71]

Figure 4 summarizes the equilibrium structures of benzyne isomers in their singlet and triplet states calculated by the SF-DFT method[92,93] in the 6-311G* basis.[94] We have also employed SF-DFT to calculate ZPEs. Two pure angular momentum basis sets are used in this subsection: 6-31G*,[95] and a basis composed of the cc-pVTZ basis on carbon and the cc-pVDZ basis on hydrogen.

Table VI shows the adiabatic energy splittings between the ground singlet state and the first excited triplet state of the benzyne isomers. With ZPE corrections, the SF-OD/6-31G* results for *o*- and *m*-benzyne are within 0.17 eV (4 kcal/mol) of the experiment,[72] and within 0.03 eV (0.7 kcal/mol) for *p*-benzyne. However, the corresponding cc-pVTZ values estimated by the energy separability formula [Eq. (12)] are within 0.03 eV (0.7 kcal/mol) of the experiment for all benzyne isomers. The SF-DFT results deviate from the experimental values by 0.22 eV (5 kcal/mol), 0.09 eV (2 kcal/mol), and 0.023 eV (0.5 kcal/mol) for *o*-, *m*-, and *p*-benzyne, respectively.

We have also calculated the vertical excitation energies for several low-lying states. Due to the extensive orbital degeneracy, the density of the excited states is rather high in benzynes. As a result, the open-shell singlet $^1B_2/^1B_{1u}$ [Eq. (3)] and the second closed-shell singlet $^1A_1/^1A_g$ [Eq. (2)] strongly interact with other excited states derived by excitation of electrons from the π system. In the energy interval from 4 to 7 eV, there are about seven states including two quintet states. The detailed results will be reported elsewhere.

E. Trimethylenemethane (TMM)

Three basis sets have been used in this section: (i) the DZP basis set;[96] (ii) a basis composed of the cc-pVTZ basis on the carbon and the cc-pVDZ on the hydrogen; and (iii) the full cc-pVTZ basis set. The SF-DFT/6-31G* method[92,93] has been used to calculate equilibrium geometries. We find that (i) the ground state SF-DFT geometry is very close to the CCSD(T) one and (ii) the relative structural changes between states are very close to those predicted by MCSCF.

TMM is an example of a non-Kekulé system: Even though it is fully conjugated, each of its Kekulé structures has at least two non-π-bonded atoms. The π system of TMM is shown in Fig. 5: four π electrons are distributed over four molecular π-type orbitals. Due to the exact degeneracy between the two e' orbitals at the D_{3h} structure, Hund rule predicts the ground state of the molecule to be a triplet $^3A_2'$ state. This is confirmed by both the experimental and theoretical findings.[45–47,70,97,98]

The vertical excited states are summarized in Table VII (C_{2v} symmetry labels are used). The three lowest states are the diradical singlet states of Eqs. (1) and (2). However, excited states that derive from excitation of other π electrons are also relatively low in energy. The first closed-shell singlet $^1A_1$ [Eq. (1)] and open-shell singlet $^1B_2$ [Eq. (3)] are degenerate at the D_{3h} geometry (because of the degeneracy of a_2 and $2b_1$ orbitals).[99] The second closed-shell singlet 2^1A_1 [Eq. (2)] is followed by a pair of degenerate triplets, $^3A_1$ and $^3B_2$, obtained by excitation of one electron from the doubly occupied $1b_1$ orbital to the a_2 or $2b_1$ degenerate orbitals.

TABLE VII. TMM. Total energies (hartree) for the ground $^3A_2'$ state and vertical excitation energies (eV) for the low-lying excited states.[a]

	$^3A_2'$	$^1A_1/^1B_2$	$2\,^1A_1$	$^3A_1/^3B_2$	$^5B_2$
SF-DFT(50/50)/6-31G*	−155.779717	1.049	3.404	6.103	
SF-CIS/DZP	−154.90553	1.154	6.627	8.428	5.712
SF-CIS(D)/DZP	−155.43585	1.160	3.821	6.018	6.729
SF-OD/DZP	−155.51414	1.198	4.000	5.941	7.221
SF-CIS/cc-pVTZ[b]	−154.91822	1.150	6.534	8.359	5.706
SF-CIS(D)/cc-pVTZ[b]	−155.54809	1.144	3.585	5.819	6.755
SF-OD/cc-pVTZ[b]	−155.62016	1.180	3.864	5.963	7.208

[a]SF-DFT/6-31G* optimized geometries (see Fig. 6).
[b]cc-pVTZ basis on carbon and cc-pVDZ basis on hydrogen.

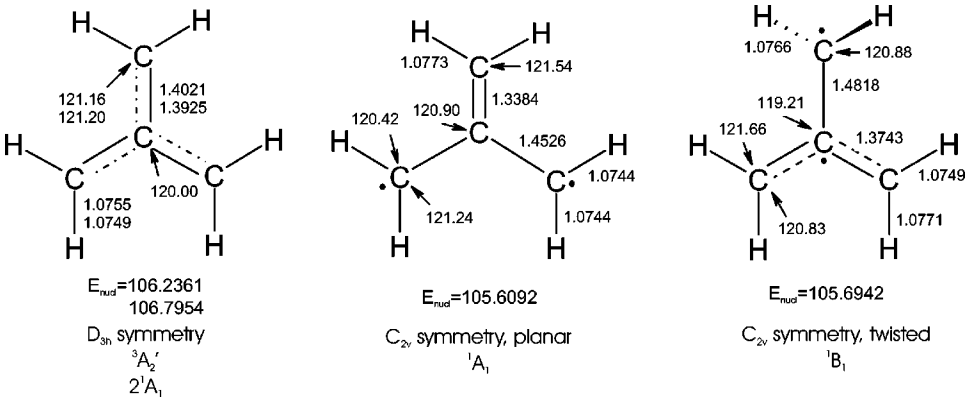

FIG. 6. Equilibrium geometries for the four lowest electronic states of TMM (bond lengths are in angstroms, angles in degrees, and nuclear repulsion energies in hartrees). Structures are optimized at the SF-DFT/6-31G* level.

Finally, there is a quintet $^5B_2$ state in which all π orbitals are singly occupied.

The equilibrium structures for the four lowest states of TMM are summarized in Fig. 6.[100] In accordance with the Jahn–Teller theorem, the degeneracy between the closed-shell and open-shell singlets can be lifted in lower symmetry. The closed-shell singlet of Ψ_1^s type is stabilized at the planar C_{2v} geometry, with one short C–C bond. The open-shell singlet of Ψ_3^s type prefers an equilibrium structure with one long C–C bond and a 90° twisted methylene group. The real minimum of the open-shell singlet is a C_s structure with a pyramidized methylene group (e.g., the dihedral angle equals 79.0°). However, the potential energy surface along the pyramidization coordinate is rather flat, i.e., the energy difference between the C_{2v} twisted and the equilibrium C_s (79.0° pyramidized) structures is only 0.001 eV (0.03 kcal/mol). Thus, for the sake of simplicity, we have used a twisted C_{2v} structure as the equilibrium geometry for the open-shell singlet $^1B_2$ (at this geometry, this state should be labeled as $^1B_1$). As mentioned in Ref. 45, this state has not been observed in the experimental photoelectron spectrum,[70] because of unfavorable Franck–Condon factors, even though adiabatically this state is the lowest singlet state.

Table VIII summarizes the adiabatic excitation energies of the three low-lying singlet states calculated by the SF and MCSCF/MCQDPT2 methods (see Fig. 6 for equilibrium geometries). Two different active spaces and three basis sets (see above) have been used in the multiconfigurational calculations. The small (4×4) active space includes four π orbitals and four electrons. The larger (10×10) active space includes six additional carbon–carbon σ and σ^* orbitals and six additional electrons participating in the C–C bonding.

TABLE VIII. TMM. Total energies (hartree) for the ground $^3A_2'$ state and adiabatic excitation energies (eV) for the low-lying excited states.[a]

	$^3A_2'$	$^1B_1$	$^1A_1$	$2\,^1A_1$
SF-DFT(50/50)/6-31G*	−155.77972	0.745	0.866	3.397
SF-CIS/DZP	−154.90553	1.018	0.882	6.616
SF-CIS(D)/DZP	−155.43585	0.987	0.885	3.826
SF-OD/DZP	−155.51414	0.697	0.936	4.023
MCSCF(4,4)/DZP	−155.936880	0.643	0.843	
MCQDPT2(4,4)/DZP	−155.423414	0.676	0.863	
MCSCF(10,10)/DZP	−155.010122	0.704	0.834	
MCQDPT2(10,10)/DZP	−155.422866	0.674	0.824	
SF-CIS/cc-pVTZ[c]	−154.91822	1.017	0.883	6.508
SF-CIS(D)/cc-pVTZ[c]	−155.54809	1.025	0.893	3.570
SF-OD/cc-pVTZ[c]	−155.62016	0.744	0.941	3.858
MCSCF(4,4)/cc-pVTZ[c]	−154.949102	0.648	0.843	
MCQDPT2(4,4)/cc-pVTZ[c]	−155.541780	0.715	0.865	
MCSCF(10,10)/cc-pVTZ[c]	−155.023549	0.708	0.833	
MCQDPT2(10,10)/cc-pVTZ[c]	−155.538683	0.715	0.830	
MCSCF(4,4)/cc-pVTZ	−154.959329	0.644	0.841	
MCQDPT2(4,4)/cc-pVTZ	−155.571449	0.711	0.862	
MCSCF(10,10)/cc-pVTZ	−155.033829	0.705	0.832	
MCQDPT2(10,10)/cc-pVTZ	−155.568282	0.710	0.828	
Expt. (Ref. 70)			0.699±0.006	
Δ ZPE[b]		−0.042	−0.088	0.026
Expt.−Δ ZPE			0.787	

[a]SF-DFT optimized geometries (see Fig. 6).
[b]Calculated at the SF-DFT/6-31G* level.
[c]cc-pVTZ basis on carbon and cc-pVDZ basis on hydrogen.

As seen from Table VIII, the MCSCF and MCQDPT2 results are very insensitive to the active space and the basis set. For the $^3A_2' \rightarrow {}^1B_1$ transition, increasing the active space changes the MCSCF excitation energy by 0.06 eV (1.4 kcal/mol), while the perturbative correction decreases the importance of the active space size and equalizes the excitation energies. For the $^3A_2' \rightarrow {}^1A_1$ transition, the situation is reverse: while the MCSCF excitation energy does not depend on active space size, the MCQDPT2 energy decreases by about 0.04 eV (0.9 kcal/mol) in a 10×10 active space. The basis set increase changes the MCQDPT2 $^3A_2' \rightarrow {}^1B_1$ excitation energy by only 0.035 eV (0.8 kcal/mol), while the $^3A_2' \rightarrow {}^1A_1$ energy is unchanged. Moreover, there is practically no difference between the mixed cc-pVTZ/cc-pVDZ and the full cc-pVTZ basis sets.

The SF-OD results differ from MCQDPT2(10×10) by 0.02 eV (0.5 kcal/mol) for the $^3A_2' \rightarrow {}^1B_1$ transition, and by 0.11 eV (2.6 kcal/mol) for the $^3A_2' \rightarrow {}^1A_1$ transition. The ZPE-corrected SF-OD results for the $^3A_2' \rightarrow {}^1A_1$ splitting deviate from the experiment by 0.15 eV (3.4 kcal/mol).

IV. CONCLUSIONS

The SF approach describes closed- and open-shell singlet and triplet states within a single reference formalism as spin-flipping, e.g., $\alpha \rightarrow \beta$, excitations from a high-spin triplet ($M_s=1$) reference state for which both dynamical and nondynamical correlation effects are much smaller than for the corresponding singlet state.[28–30] In this work, several SF models of increased complexity have been applied to calculate vertical and adiabatic energy separations between low-lying states of diradicals. Due to the single-reference nature of the high-spin triplet diradical states, the SF models yield systematically more accurate results than their traditional (non-SF) counterparts. Our results demonstrate that the SF approach extends the scope of applicability of single-reference methods from well-behaved systems (e.g., closed-shell molecules around the equilibrium geometries) to situations plagued by electronic degeneracy, e.g., diradicals and bond-breaking.

For all the diradicals considered here, the SF variant of the EOM-OD model yields energy separations that are within less than 3 kcal/mol of the experimental or the highly accurate MR values. In most cases the errors are about 1 kcal/mol. Drawing from the performance of single-reference methods for well-behaved molecules, we expect that a perturbative account of triple excitations will bring the corresponding SF-CC model into the *chemical accuracy*, i.e., <1 kcal/mol, range. The less computationally demanding SF-CIS(D) model consistently yields results that are within 0.1–0.25 eV of the SF-OD ones. Moreover, SF-CIS(D) can be used to extrapolate the large basis set results of the more computationally expensive SF-CC methods.

Regarding comparison with MR techniques, the following advantages of the SF approach are particularly attractive: (i) lower computational cost and scaling;[101] (ii) the multistate nature of the SF method, i.e., its ability to calculate several excited states at once, rather than in a state-by-state fashion; (iii) simpler formalism, e.g., the analytic gradient theory is rather straightforward for the SF models—in spin-orbital formulation, it is identical to the corresponding non SF theories;[102–105] (iv) the ''black-box'' nature of the (single-reference) SF methods which do not involve active space and/or configurations selection.

ACKNOWLEDGMENTS

Support from the National Science Foundation CAREER Award (Grant No. CHE-0094116), the Camille and Henry Dreyfus New Faculty Awards Program, and the Donors of the Petroleum Research Fund administered by the American Chemical Society is gratefully acknowledged. We thank Yihan Shao for sharing his results prior to publication.

[1] L. Salem and C. Rowland, Angew. Chem. Int. Ed. Engl. **11**, 92 (1972).
[2] N. Turro, *Modern Molecular Photochemistry* (Benjamin/Cummings, Menlo Park, California, 1978).
[3] *Diradicals* edited by W. T. Borden (Wiley, New York, 1982).
[4] V. Bonačić-Koutecký, J. Koutecký, and J. Michl, Angew. Chem. Int. Ed. Engl. **26**, 170 (1987).
[5] *Kinetics and Spectroscopy of Carbenes and Biradicals*, edited by M. S. Platz (Plenum Press, New York, 1990).
[6] For example, when orbitals ϕ_1 and ϕ_2 are exactly degenerate (as are π and π^* in 90° twisted ethylene), the determinants (a) and (b) from Fig. 1 contribute equally to Ψ_1^s and Ψ_2^s, i.e., $\lambda=1/\sqrt{2}$. By substituting $\pi=(1/\sqrt{2})(p_A+p_B)$ and $\pi^*=(1/\sqrt{2})(p_A-p_B)$ in Eqs. (1) and (2), the spatial parts of Ψ_1^s and Ψ_2^s become: $\Psi_1^s=1/\sqrt{2}\,(p_Ap_B+p_Bp_A)$ and $\Psi_2^s=1/\sqrt{2}\,(p_Ap_A+p_Bp_B)$, where $p_{A,B}$ denote p orbitals centered on the two carbons of ethylene. Thus, the wave function Ψ_1^s is purely covalent, whereas Ψ_2^s is ionic.
[7] B. O. Roos, P. R. Taylor, and P. E. M. Siegbahn, Chem. Phys. **48**, 157 (1980).
[8] K. Ruedenberg, M. W. Schmidt, M. M. Gilbert, and S. T. Elbert, Chem. Phys. **71**, 41 (1982).
[9] See articles by B. O. Roos; P. Bruna and S. D. Peyerimhoff; R. Shepard; and D. L. Cooper, J. Gerratt, and M. Raimondi, in *Ab Initio Methods in Quantum Chemistry, II* (Wiley, New York, 1987).
[10] K. Andersson, P.-Å. Malmqvist, B. O. Roos, A. J. Sadlej, and K. Wolinski, J. Phys. Chem. **94**, 5483 (1990).
[11] K. Andersson, P.-Å. Malmqvist, and B. O. Roos, J. Chem. Phys. **96**, 1218 (1992).
[12] H. Nakano, J. Chem. Phys. **99**, 7983 (1993).
[13] *Recent Advances in Multi-Reference Methods*, edited by K. Hirao (World Scientific, Singapore, 1999).
[14] M. Nooijen, Int. J. Mol. Sci. (to be published).
[15] M. Wladyslawski and M. Nooijen, *ACS Conference Proceedings* (to be published).
[16] E. R. Davidson, J. Phys. Chem. **100**, 6161 (1996).
[17] P. M. Kozlowski, M. Dupuis, and E. R. Davidson, J. Am. Chem. Soc. **117**, 774 (1995).
[18] W. T. Borden and E. R. Davidson, Acc. Chem. Res. **29**, 67 (1996).
[19] N. W. Moriarty, R. Lindh, and G. Karlsröm, Chem. Phys. Lett. **289**, 442 (1998).
[20] Ideally, one would like to always employ a full valence active space (bonding, antibonding, and lone pair orbitals). Such active space is uniquely defined, and the corresponding CASSCF wave function is flexible enough to describe all the major interactions of the valence electrons, e.g., the polarization of σ electrons for the $\pi\pi^*$ ionic configurations, as in the V state of ethylene (Refs. 16 and 18), etc. Unfortunately, the computational cost, which grows factorially with molecular size, rapidly makes this approach unfeasible for systems of more than two or three heavy atoms. The most common approximation involves reduction of the active space guided by physical considerations, which are specific for each particular species or reaction. In addition to the certain arbitrariness of such an approach, the small active space can seriously affect the quality of the resulting wave function, even when dynamical correlation is included in MRCI or MRPT fashion. For example, a recent study of tetramethylene (Ref. 19) has demonstrated that the selection of the active space for the CASSCF wave function strongly influences the shape of the PES even at the CASPT2 level (the existence of some stationary points

calculated at the lower level of theory was not confirmed by more accurate calculations). Recently, alternative approximations to the full valence space CASSCF have been introduced [A. I. Krylov, C. D. Sherrill, E. F. C. Byrd, and M. Head-Gordon, J. Chem. Phys. **109**, 10 669 (1998); S. R. Gwattney, C. D. Sherrill, M. Head-Gordon, and A. I. Krylov, *ibid.* **113**, 3548 (2000)].
[21] I. Tamm, J. Phys. USSR **9**, 449 (1945).
[22] J. A. Pople, Trans. Faraday Soc. **49**, 1375 (1953).
[23] J. B. Foresman, M. Head-Gordon, J. A. Pople, and M. J. Frisch, J. Phys. Chem. **96**, 135 (1992).
[24] M. Head-Gordon, R. J. Rico, M. Oumi, and T. J. Lee, Chem. Phys. Lett. **219**, 21 (1994).
[25] H. Koch, H. Jørgen, Aa. Jensen, and P. Jørgensen, J. Chem. Phys. **93**, 3345 (1990).
[26] J. F. Stanton and R. J. Bartlett, J. Chem. Phys. **98**, 7029 (1993).
[27] A. I. Krylov, C. D. Sherrill, and M. Head-Gordon, J. Chem. Phys. **113**, 6509 (2000).
[28] A. I. Krylov, Chem. Phys. Lett. **338**, 375 (2001).
[29] A. I. Krylov and C. D. Sherrill, J. Chem. Phys. **116**, 3194 (2002).
[30] A. I. Krylov, Chem. Phys. Lett. **350**, 522 (2001).
[31] K. B. Eisenthal, R. A. Moss, and N. J. Turro, Science **225**, 1439 (1984).
[32] This can have far reaching consequences: for example, unlike triplet species, singlet *p*-benzynes have been shown to selectively cleave DNA [J. Hoffner, M. J. Schottelius, D. Feichtinger, and P. Chen, J. Am. Chem. Soc. **120**, 376 (1998); G. F. Logan and P. Chen, *ibid.* **118**, 213 (1996); M. J. Schottelius and P. Chen, *ibid.* **118**, 4896 (1996); M. J. Schottelius and P. Chen, Angew. Chem. Int. Ed. Engl. **3**, 1478 (1996)], thus suggesting their use as antitumor agents [*Enediyne Antibiotics as Antitumor Agents*, edited by D. B. Borders and T. W. Doyle (Dekker, New York, 1995); *Neocarzinostatin: The Past, Present, and Future of an Anticancer Drugs* edited by H. Maeda, K. Edo, and N. Ishida (Springer, New York, 1997)].
[33] Y. Yamaguchi, C. D. Sherrill, and H. F. Schaefer III, J. Phys. Chem. **100**, 7911 (1996).
[34] J. C. Stefens, Y. Yamaguchi, C. D. Sherrill, and H. F. Schaefer III, J. Phys. Chem. **102**, 3999 (1998).
[35] Y. Yamaguchi, T. J. Van Huis, C. D. Sherrill, and H. F. Schaefer III, Theor. Chem. Acc. **97**, 341 (1997).
[36] T. J. Van Huis, Y. Yamaguchi, C. D. Sherrill, and H. F. Schaefer III, J. Phys. Chem. **101**, 6955 (1997).
[37] C. J. Cramer, F. J. Dulles, J. W. Storer, and S. E. Worthington, Chem. Phys. Lett. **218**, 387 (1994).
[38] C. W. Bauschlicher, S. R. Langhoff, and P. R. Taylor, J. Chem. Phys. **87**, 387 (1987).
[39] K. Balasubramanian and A. D. McLean, J. Chem. Phys. **85**, 5117 (1986).
[40] J. Karolczak, W. W. Harper, R. S. Grev, and D. J. Clouthier, J. Chem. Phys. **103**, 2839 (1995).
[41] K. Balasubramanian, Y. S. Chung, and W. S. Glaunsinger, J. Chem. Phys. **98**, 8859 (1993).
[42] R. R. Squires and C. J. Cramer, J. Phys. Chem. **102**, 9072 (1998).
[43] C. J. Cramer, J. J. Nash, and R. R. Squires, Chem. Phys. Lett. **277**, 311 (1997).
[44] H. F. Bettinger, P. v. R. Schleyer, and H. F. Schaefer III, J. Am. Chem. Soc. **121**, 2829 (1999).
[45] C. J. Cramer and B. A. Smith, J. Physiol. (London) **100**, 9664 (1996).
[46] D. Feller, K. Tanaka, E. R. Davidson, and W. T. Borden, J. Am. Chem. Soc. **104**, 967 (1982).
[47] E. R. Davidson and W. T. Borden, J. Am. Chem. Soc. **99**, 2053 (1977).
[48] S. B. Lewis, D. A. Hrovat, S. J. Getty, and W. T. Borden, J. Chem. Soc., Perkin Trans. **1999**, 2339.
[49] E. A. Carter and W. A. Goddard III, J. Chem. Phys. **88**, 1752 (1988).
[50] D. A. Hrovat, K. Morokuma, and W. T. Borden, J. Am. Chem. Soc. **116**, 1072 (1994).
[51] S. Wilsey, K. N. Houk, and A. H. Zewail, J. Am. Chem. Soc. **121**, 5772 (1999).
[52] M. Prall, A. Wittkopp, and P. R. Schreiner, J. Phys. Chem. A **105**, 9265 (2001).
[53] P. R. Schreiner and M. Prall, J. Am. Chem. Soc. **121**, 8615 (1999).
[54] R. A. Chiles and C. E. Dykstra, J. Chem. Phys. **74**, 4544 (1981).
[55] N. C. Handy, J. A. Pople, M. Head-Gordon, K. Raghavachari, and G. W. Trucks, Chem. Phys. Lett. **164**, 185 (1989).
[56] J. Gräfenstein, E. Kraka, and D. Cremer, Chem. Phys. Lett. **288**, 593 (1998).
[57] M. Filatov and S. Shaik, Phys. Chem. A **104**, 6628 (2000).
[58] J. Gräfenstein and D. Cremer, Phys. Chem. Chem. Phys. **2**, 2091 (2000).
[59] T. Helgaker, P. Jørgensen, and J. Olsen, *Molecular Electronic Structure Theory* (Wiley, New York, 2000).
[60] C. D. Sherrill, M. L. Leininger, T. J. Van Huis, and H. F. Schaefer III, J. Chem. Phys. **108**, 1040 (1998).
[61] P. Jensen and P. R. Bunker, J. Chem. Phys. **89**, 1327 (1998).
[62] S. Gibson, J. Greene, and J. Berkowitz, J. Chem. Phys. **83**, 4319 (1985).
[63] J. Berkowitz, J. P. Greene, H. Cho, and B. Ruscic, J. Chem. Phys. **86**, 1235 (1987).
[64] J. Berkowitz and H. Cho, J. Chem. Phys. **90**, 1 (1989).
[65] W. H. Green Jr., N. C. Handy, P. J. Knowles, and S. Carter, J. Chem. Phys. **94**, 118 (1991).
[66] R. Escribano and A. Campargue, J. Chem. Phys. **108**, 6249 (1998).
[67] K. P. Huber and G. Herzberg, *Constants of Diatomic Molecules* (Van Nostrand Reinhold, New York, 1979).
[68] P. Dowd, Acc. Chem. Res. **5**, 242 (1972).
[69] D. Dougherty, Acc. Chem. Res. **24**, 88 (1991).
[70] P. G. Wenthold, J. Hu, R. R. Squires, and W. C. Lineberger, J. Am. Chem. Soc. **118**, 475 (1996).
[71] T. D. Crawford, E. Kraka, J. F. Stanton, and D. Cremer, J. Chem. Phys. **114**, 10638 (2001).
[72] P. G. Wenthold, R. R. Squires, and W. C. Lineberger, J. Am. Chem. Soc. **120**, 5279 (1998).
[73] This formula has been proposed for the extrapolation of *correlation* energy. However, it is unclear how to define correlation energy in the EOM methods. One possibility is to define correlation energy as a difference between the total energy of the final state and the Hartree–Fock energy of the (triplet) reference state. We have found that in this case the resulting ΔE_{ST} values differ from the ones obtained by extrapolating the total energies by no more than 0.001 eV.
[74] D. Feller, J. Chem. Phys. **96**, 6104 (1992).
[75] K. A. Peterson and T. H. Dunning, Jr., J. Chem. Phys. **102**, 2032 (1995).
[76] K. A. Peterson, D. E. Woon, and T. H. Dunning, Jr., J. Chem. Phys. **100**, 7410 (1994).
[77] D. E. Woon, K. A. Peterson, and T. H. Dunning, Jr., J. Chem. Phys. **109**, 2233 (1998).
[78] J. Kong, C. A. White, A. I. Krylov *et al.*, J. Comput. Chem. **21**, 1532 (2000).
[79] T. D. Crawford, C. D. Sherrill, E. F. Valeev *et al.*, PSI 3.0, PSITECH, Inc., Watkinsville, GA 30677, 1999.
[80] J. F. Stanton, J. Gauss, J. D. Watts, W. J. Lauderdale, and R. J. Bartlett, ACES II, 1993. The package also contains modified versions of the MOLECULE Gaussian integral program of J. Almlöf and P. R. Taylor, the ABACUS integral derivative program written by T. U. Helgaker, H. J. Aa. Jensen, P. Jørgensen and P. R. Taylor, and the PROPS property evaluation integral code of P. R. Taylor.
[81] M. W. Schmidt, K. K. Baldridge, J. A. Boatz *et al.*, J. Comput. Chem. **14**, 1347 (1993).
[82] Basis sets were obtained from the Extensible Computational Chemistry Environment Basis Set Database, Version, as developed and distributed by the Molecular Science Computing Facility, Environmental and Molecular Sciences Laboratory which is part of the Pacific Northwest Laboratory, P.O. Box 999, Richland, Washington 99352, and funded by the U.S. Department of Energy. The Pacific Northwest Laboratory is a multiprogram laboratory operated by Battelle Memorial Institute for the U.S. Department of Energy under Contract No. DE-AC06-76RLO 1830. Contact David Feller or Karen Schuchardt for further information.
[83] The DZP basis for carbon and oxygen is defined by Dunning's double-ζ contraction [T. H. Dunning, J. Chem. Phys. **53**, 2823 (1970)] of Huzinaga's primitive Gaussian functions [S. Huzinaga, J. Phys. Chem. **42**, 1293 (1965)] and a single set of polarization functions [α_d(C)=0.75, α_d(O)=0.85], the contraction scheme being $(9s5p1d/4s2p1d)$. The triple-ζ (TZ) Huzinaga-Dunning bases [Ref. 15; T. H. Dunning, J. Chem. Phys. **55**, 716 (1971)] [contraction schemes are $(10s6p/5s3p)$ for carbon and oxygen, and $(12s9p/6s5p)$ for silicon] are augmented by: (i) two sets of polarization functions (TZ2P) [α_d(C)=1.50, 0.375; α_d(O)=1.70, 0.4250; α_d(Si)=1.00, 0.25]; (ii) three sets of polarization functions (TZ3P) [α_d(C)=3.00, 0.75,0.1875; α_d(O)=3.40, 0.85,0.2125]. Then additional sets of f functions are added: (i) one set of f functions for TZ2P (TZ2PF) [α_f(C)=0.80; α_f(O)=1.40]; (ii) two sets of f functions for TZ3P (TZ3P2F) [α_f(C)=1.60, 0.40; α_f(O)=2.80, 0.70]. In addition, TZ2P and TZ2PF bases augmented by one set of diffuse functions (TZ2P+diff and TZ2PF+diff, respectively) are considered [α_s(C)=0.04812, α_p(C)=0.03389; α_s(O)=0.08993, α_p(O)=0.0584; α_s(Si)=0.02567, α_p(Si)

=0.02354]. Cartesian d and f functions are used for carbon and oxygen, and pure angular momentum for silicon. In addition, series of correlation consistent basis sets (cc-pVDZ, cc-pVTZ, and cc-pVQZ [Ref. 90; D. Wooh and T. H. Dunning (to be published)]) are used (these employ pure angular momentum d-, f-, and g-functions).

[84] A. D. Walsh, J. Chem. Soc. **1953**, 2260.

[85] The TZ bases for carbon and hydrogen are from Refs. 33 and 60; for nitrogen from Ref. 34. The TZ bases for silicon and phosphorus are from Refs. 35 and 36, respectively. All carbon bases are the same as in the previous section. However, some labels are slightly different: i.e., TZ2P(f,d) and TZ3P(2 f,2d) are equivalent to TZ2PF and TZ3P2F from Sec. III A. The TZ-quality basis sets for hydrogen and nitrogen are derived from the Huzinaga–Dunning basis [S. Huzinaga, J. Chem. Phys. **42**, 1293 (1965) and T. H. Dunning, J. Chem. Phys. **55**, 716 (1971)], the contraction scheme being (10s6p/5s3p) for N, and (5s/3s) for H. The TZ-quality bases for silicon and phosphorus are defined by the McLean-Chandler TZ contraction [A. D. McLean and G. S. Chandler, J. Chem. Phys. **72**, 5639 (1980)] of the Huzinaga's primitive Gaussian functions [S. Huzinaga, *Approximate Atomic Wave Functions*, Vol. II, University of Alberta, Alberta, (1971)]: the contraction scheme is (12s9p/6s5p) for Si and P. We augment these basis sets by: (i) two sets of polarization functions (TZ2P) [α_p(H)=1.50, 0.375; α_d(N)=1.60, 0.40; α_d(Si)=1.00, 0.25 and α_d(P)=1.20, 0.30]; (ii) three sets of polarization function, TZ3P(2 f,2d) [α_p(H)=3.00, 0.75, 0.1875]. The orbital exponents of higher angular momentum functions are: (i) α_d(H)=1.00, α_f(N)=1.00, α_f(Si)=0.32 and α_f(P)=0.45 for a single set of higher angular momentum functions [TZ2P(f,d) bases] and (ii) α_d(H)=2.00,0.50 for a double set of higher angular momentum functions [TZ3P(2 f,2d)]. In addition, the TZ2P and TZ2P(f,d) bases are augmented by one set of diffuse functions [TZ2P+diff and TZ2P(f,d)+diff, respectively], with the exponent α_s(H)=0.03016 (diffuse functions on heavy atoms are the same as in the previous section). Lastly, correlation-consistent basis sets have been employed, i.e., cc-pVDZ, cc-pVTZ, and cc-pVQZ [Refs. 90 and D. Wooh and T. H. Dunning (to be published)]. Pure angular momentum d, f, and g functions are used in all the calculations reported in this section.

[86] To calculate adiabatic energy separations in methylene, FCI/TZ2P optimized geometries (Ref. 60) are used (r_e in Å/Θ_e in degree): 1.0775/133.29, 1.1089/101.89, 1.0748/141.56, and 1.0678/170.08 for the $\tilde{X}\,^3B_1$, $\tilde{a}\,^1A_1$, $\tilde{b}\,^1B_1$, and $\tilde{c}\,^1A_1$ states, respectively. The equilibrium geometries for NH_2^+ are CISD/TZ2P(f,d) optimized geometries (Ref. 34): 1.0295/150.88, 1.0459/107.96, 1.0293/161.47, and 1.0315/180.00 for the $\tilde{X}\,^3B_1$, $\tilde{a}\,^1A_1$, $\tilde{b}\,^1B_1$, and $\tilde{c}\,^1A_1$ states, respectively. For SiH_2 and PH_2^+, we employ the CISD/TZ2P(f,d) optimized geometries from Refs. 35 and 36, respectively. The equilibrium structures of the $\tilde{X}\,^1A_1$, $\tilde{a}\,^3B_1$, $\tilde{A}\,^1B_1$, and $\tilde{B}\,^1A_1$ states of SiH_2 are 1.5145/92.68, 1.4770/118.26, 1.4830/122.65, and 1.4573/162.34, respectively. For PH_2^+, geometries of these states are: 1.4178/93.06, 1.4056/121.77, 1.4194/124.84, and 1.4118/159.62.

[87] H. Petek, D. J. Nesbitt, D. C. Darwin, P. R. Ogilby, C. B. Moore, and D. A. Ramsay, J. Chem. Phys. **91**, 6566 (1989).

[88] G. Duxbury and C. Jungen, Mol. Phys. **63**, 981 (1988).

[89] In variational methods, the energy of an approximate wave function can be lowered by breaking its spin or point group symmetry. Thus, for any variational model (e.g., Hartree-Fock or CI), energies of spin-contaminated solutions are always lower than those of the spin-pure ones. Rigorously, this may not be the case for non-variational methods such as CCSD or B-CCD. Practically, however, spin-contaminated energies are usually lower than spin-pure ones for non-variational methods as well. Spin-contamination of coupled-cluster wave functions has been recently discussed by A. I. Krylov, J. Chem. Phys. **113**, 6052 (2000).

[90] T. H. Dunning, J. Chem. Phys. **90**, 1007 (1989).

[91] The following equilibrium bond lengths for the $^1\Delta$ and $^3\Sigma$ states are used (Ref. 67): 1.034 and 1.036 Å for NH; 1.308 and 1.317 Å for NF; 1.215 and 1.207 Å for O_2. For OH^+, the experimental geometry of the $^3\Sigma$ state (r_e=1.029 Å) is used for both states [theoretical calculations (Ref. 56) predict that the difference in the r_e of these states is very small, i.e. $\approx$0.001 Å].

[92] A. I. Krylov, Y. Shao, and M. Head-Gordon (unpublished).

[93] We used the functional composed of the equal mixture of the following exchange and correlation parts: 50% Hartree–Fock+8% Slater +42% Becke for exchange, and 19% VWN+81% LYP for correlation.

[94] R. Krishnan, J. S. Binkley, R. Seeger, and J. A. Pople, J. Chem. Phys. **72**, 650 (1980).

[95] P. C. Hariharan and J. A. Pople, Theor. Chim. Acta **28**, 213 (1973).

[96] The DZP basis for carbon is the same as in Sec. III A. The DZP basis for hydrogen is a Huzinaga–Dunning [S. Huzinaga, J. Chem. Phys. **42**, 1293 (1965) and T. H. Dunning, J. Chem. Phys. **53**, 2823 (1970)] basis augmented by a single set of polarization functions [α_p(H)=1.00]. Pure angular momentum d functions are used.

[97] P. Dowd, J. Am. Chem. Soc. **88**, 2587 (1966).

[98] R. J. Baseman, D. W. Pratt, M. Chow, and P. Dowd, J. Am. Chem. Soc. **98**, 5726 (1976).

[99] This is similar to the NH_2^+ diradical at linear geometry where the $\tilde{a}\,^1A_1$ and $\tilde{b}\,^1B_1$ states become degenerate as two components of the $^1\Delta_g$ state.

[100] Note that the PES of the open-shell singlet has no minimum at the C_{2v} planar structure. Likewise, the PES of the triplet state has no minimum at the C_{2v} 90° twisted structure. This can be demonstrated by the vibrational analysis which yields one imaginary frequency corresponding to the rotation of methylene group for the structures obtained by the constrained optimization. We do not discuss these saddle points, even though these structures have been previously reported (Ref. 45).

[101] The scaling of the spin-orbital implementation of the SF-CIS model is N^5 (due to integral transformation); however, it can easily be reduced to approximately N^2 by implementing the direct algorithm for the CIS procedure (Ref. 78). The scaling of the SF-CIS(D) model is N^5, and the N^5 step is noniterative. Similar to their non SF counterparts, the SF-CISD, SF-CCSD, and SF-OD models scale as N^6. The scaling of MR models is factorial due to the MCSCF part. The scaling bottleneck restricts full valence space MCSCF calculations to systems of just two or three heavy atoms. For example, the full valence active space for TMM consists of 16 orbitals and contains 16 electrons. It is not yet possible to carry out such calculations with today's hardware and software tools. As far as timing is considered, the comparison between MR and SF models is more difficult since the absolute timing strongly depends upon implementation.

[102] J. F. Stanton, J. Chem. Phys. **99**, 8840 (1993).

[103] J. F. Stanton and J. Gauss, Theor. Chem. Acc. **91**, 267 (1995).

[104] J. F. Stanton, J. Gauss, N. Ishikawa, and M. Head-Gordon, J. Chem. Phys. **103**, 4160 (1995).

[105] K. K. Baek, J. Chem. Phys. **112**, 1 (2000).